

# High sensitivity heat capacity measurements on $\text{Sr}_2\text{RuO}_4$ under uniaxial pressure

You-Sheng Li<sup>a,b</sup>, Naoki Kikugawa<sup>c</sup>, Dmitry A. Sokolov<sup>a</sup>, Fabian Jerzembeck<sup>a</sup>, Alexandra S. Gibbs<sup>d</sup>, Yoshiteru Maeno<sup>e</sup>, Clifford W. Hicks<sup>a</sup>, Jörg Schmalian<sup>f,g</sup>, Michael Nicklas<sup>a,1</sup>, and Andrew P. Mackenzie<sup>a,b,1</sup>

<sup>a</sup>Max Planck Institute for Chemical Physics of Solids, Nöthnitzer Str. 40, 01187 Dresden, Germany; <sup>b</sup>Scottish Universities Physics Alliance, School of Physics and Astronomy, University of St Andrews, St Andrews, UK; <sup>c</sup>National Institute for Materials Science, Tsukuba 305-0003, Japan; <sup>d</sup>ISIS facility, STFC Rutherford Appleton Laboratory, Chilton, Didcot, OX11 0QX, UK; <sup>e</sup>Department of Physics, Graduate School of Science, Kyoto University, Kyoto, Japan; <sup>f</sup>Institut für Theorie der Kondensierten Materie, Karlsruher Institut für Technologie, 76131 Karlsruhe, Germany; <sup>g</sup>Institut für Quantenmaterialien und -technologien, Karlsruher Institut für Technologie, 76131 Karlsruhe, Germany

This manuscript was compiled on January 13, 2021

**A key question regarding the unconventional superconductivity of  $\text{Sr}_2\text{RuO}_4$  remains whether the order parameter is single- or two-component. Under a hypothesis of two-component superconductivity, uniaxial pressure is expected to lift their degeneracy, resulting in a split transition. The most direct and fundamental probe of a split transition is heat capacity. Here, we report measurement of heat capacity of samples subject to large and highly homogeneous uniaxial pressure. We place an upper limit on the heat-capacity signature of any second transition of a few per cent of that of the primary superconducting transition. The normalized jump in heat capacity,  $\Delta C/C$ , grows smoothly as a function of uniaxial pressure, favouring order parameters which are allowed to maximize in the same part of the Brillouin zone as the well-studied van Hove singularity. Thanks to the high precision of our measurements, these findings place stringent constraints on theories of the superconductivity of  $\text{Sr}_2\text{RuO}_4$ .**

Obtaining a full understanding of the superconductivity of  $\text{Sr}_2\text{RuO}_4$  is a core challenge for condensed matter physics. Since soon after its discovery over a quarter of a century ago (1), the superconducting order parameter of  $\text{Sr}_2\text{RuO}_4$  has been known to be unconventional (2, 3), and to condense from a well-understood and fairly simple quasi-two-dimensional Fermi liquid metallic state (4–7). Given the profound advances in theoretical techniques in recent decades a full understanding of its superconductivity is an important, and attainable, challenge for the field. The form of the wave-vector dependent susceptibility of  $\text{Sr}_2\text{RuO}_4$  leads to the prediction of a rich superconducting phase diagram in weak-coupling calculations which aim to perform a bias-free estimate of the condensation energies of different order parameters. A notable feature of the results is how close a number of different odd- and even-parity solutions are seen to be in energy (8–10). On the one hand this emphasizes the potential of  $\text{Sr}_2\text{RuO}_4$  as a test-bed material on which to refine the predictive capabilities of modern theories of unconventional superconductivity (11). On the other hand, realising this potential will likely first require a conclusive experimental determination of which of the many possible order parameters wins out in the real material. This is a particularly exciting stage of the quest to complete this empirical determination, for reasons that we will now outline.

For over twenty years, the large majority of attention was paid to odd-parity order parameter candidates for  $\text{Sr}_2\text{RuO}_4$  (12), because of nuclear magnetic resonance (NMR) measurements of spin susceptibility in the superconducting state that seemed to be inconsistent with any even-parity order parameter (13). However, thanks to the discovery of a systematic error in the original NMR measurements (14, 15), that situa-

tion has now been more or less completely reversed. Taking into account the most recent measurements of the magnetic field dependence of the spin susceptibility (16), it seems clear that the order parameter must be even parity or at least dominated by an even parity component. The spin susceptibility results would be most easily describable in terms of a single-component, likely *d*-wave, order parameter, but recent thermodynamic evidence from ultrasound experiments is most straightforwardly interpreted in terms an order parameter with two degenerate components (17, 18). Such order parameters do not of necessity break time-reversal symmetry, but they can, if the two degenerate have the appropriate phase relationship. In the context it is significant that long-standing muon-spin relaxation ( $\mu\text{SR}$ ) (19, 20) and magneto-optic Kerr rotation measurements (21) have indicated time-reversal symmetry breaking in the superconducting state.

To investigate any order parameter with two degenerate components, whether or not it breaks time-reversal symmetry, uniaxial pressure is a powerful probe because it can split the degeneracy, creating a split superconducting phase transition (22). In a significant experimental advance, the muon-spin relaxation experiments have recently been extended to high uniaxial pressures (23). In line with naive expectation, the tem-

## Significance Statement

Research on the unconventional superconductivity of  $\text{Sr}_2\text{RuO}_4$  is undergoing a renaissance since recent spin susceptibility measurements ruling out the spin triplet order parameter which had been widely favored for over two decades. With ultrasound, Kerr rotation and muon spin relaxation data all providing evidence for a two-component order parameter, it is vital that this possibility be investigated thermodynamically by studying the dependence of the heat capacity anomaly on uniaxial pressure. Here, the relevant experimental results are combined with theoretical analysis that shows how strongly the data constrain theories of the order parameter. In particular, we do not observe any signs of transition splitting of two order parameter components.  $\text{Sr}_2\text{RuO}_4$  thus offers a unique test-bed for theories of unconventional superconductivity.

The idea to try this programme of research came from M.N., and the appropriate experimental apparatus was conceived by M.N. and C.W.H. and developed by Y.-S.L.. The large majority of the experiments and data analysis was performed by Y.-S.L. with contributions from M.N., C.W.H. and F.J., on crystals grown and characterized by N.K., A.S.G., D.A.S., F.J. and Y.M.. A.P.M. oversaw the complete project and drafted the paper, with input from Y.-S.L., M.N., C.W.H., J.S. and Y.M..

The authors declare no conflict of interest.

<sup>1</sup>To whom correspondence should be addressed. E-mail: Michael.Nicklas@cpfs.mpg.de or Andy.Mackenzie@cpfs.mpg.de

perature at which time-reversal symmetry is broken ( $T_{TRSB}$ ) splits from the main superconducting transition ( $T_c$ ), with  $T_{TRSB}$  remaining nearly pressure-independent while  $T_c$  increases under the application of the pressure. However, there has been a long-standing question about whether the Kerr and muon signals correspond to bulk thermodynamic transitions, so it is highly desirable to compare the new muon-spin relaxation data with those from a bulk thermodynamic probe. In this context, it is natural to look at heat capacity, because it has an intrinsic sensitivity to transitions within the superconducting state, as is well known from work on  $UPT_3$  (24, 25).

## Experiment

Both for the above reasons and to give the now widely applied uniaxial pressure measurements a solid thermodynamic foundation, we have developed a high-frequency ac technique for measuring heat capacity in a uniaxial pressure cell. Full technical details are given in (26); here we summarise the governing relationship of the measurement:

$$C_{ac} = \frac{P}{\omega T_{ac}} F(\omega), \quad [1]$$

where  $T_{ac}$  is the measured amplitude of the temperature oscillation in response to an oscillatory heat input,  $P$  is the power associated with that heat input, and  $\omega$  is the angular frequency.  $F(\omega)$  is the frequency response curve that characterizes the thermalization of the sample, and depends on the time constants, thermal conductances and heat capacities of the system. In the very high frequency version of the technique that we employ to restrict the probed volume to the most homogeneously strained central portion of the sample, the probed volume depends on the sample's thermal conductivity. The quantity  $P/(\omega T_{ac})$  is therefore closely related, but not identical, to the intrinsic heat capacity of the sample. This is not a major restriction because the sensitivity of the measurement to phase transitions is hardly affected, and robust analysis of important quantities such as the ratio of the heat capacity jump to the normal state heat capacity can still be carried out. However, to emphasize that these are not fully calibrated measurements of the full sample heat capacity, we begin by showing unprocessed experimental data.

## Results

In Figs. 1A and 1B we display raw data for  $P/(\omega T_{ac})$  as a function of temperature for strains below and above that at which  $T_c$  of  $Sr_2RuO_4$  is maximized. A background signal exists, but this can straightforwardly be identified by the application of a magnetic field of 0.1 T at zero applied pressure (dotted black line in Fig. 1A). Data toward lower temperatures can be found in the *Supporting Information, Heat Capacity Measurements in the Temperature Range between 0.5 and 4 K*. That it is essentially independent of the strain in the sample is demonstrated by how closely it is followed at all temperatures above  $T_c$ , for all strains (Figs. 1A and 1B). The heat capacity anomaly associated with superconductivity is clearly visible in the raw data, and identifying  $T_c$  from the leading edge of the anomaly allows its strain dependence to be plotted in Fig. 1C. It is seen to be in excellent agreement with previous determinations based on magnetic susceptibility (27, 28); the current

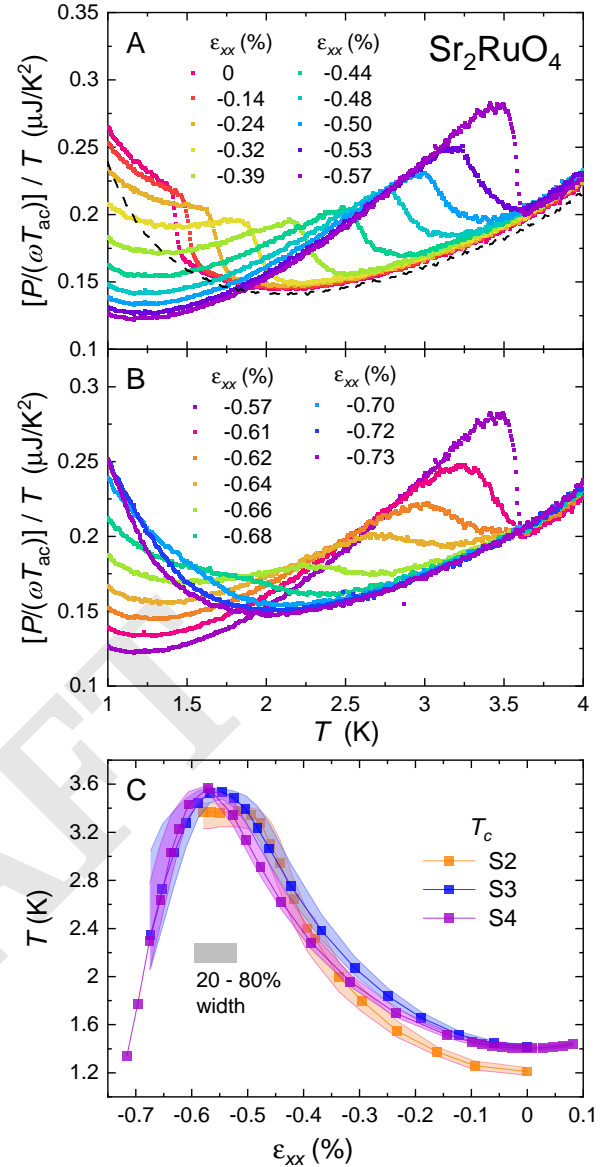


**Fig. 1.** (A) Experimental heat capacity data for strains between zero and  $\epsilon_{xx} = 0.57\%$  and (B) for  $\epsilon_{xx} \geq 0.57\%$ .  $P$  is the applied heater power and  $T_{ac}$  the temperature oscillation amplitude in response; for further explanation, see the main text. The dashed line in panel (A) is a measurement at  $\mu_0 H_{||c} = 0.1$  T and  $\epsilon_{xx} = 0$ . (C) The transition temperatures as a function of strain for three different samples, extracted from the leading edges of the superconducting anomalies, based on data taken at similar frequencies (3.5 kHz for sample S2 and 3.9 kHz for samples S3, S4). The solid points are based on the midpoints (50%) of the leading edge, and the shading represents the breadth of the transition from the 20% to 80% levels.

data fully confirm that it is a bulk phenomenon. Although we refer to (26) for the details of all the experimental steps necessary to obtain data of the quality shown in Fig. 1, we note in passing that the required specifications were demanding, and in particular that low temperature amplification was employed to reduce the voltage noise on the thermocouple reading used to determine  $T_{ac}$  to less than  $20 \text{ pVHz}^{-1/2}$ .

It was also possible to study the magnetic field dependence of the heat capacity anomaly with high precision, as is demonstrated in Figs. 2A and B for unstrained and  $T_c$ -maximized samples respectively. We note that in Fig. 2  $P/(\omega T_{ac})$  is nor-

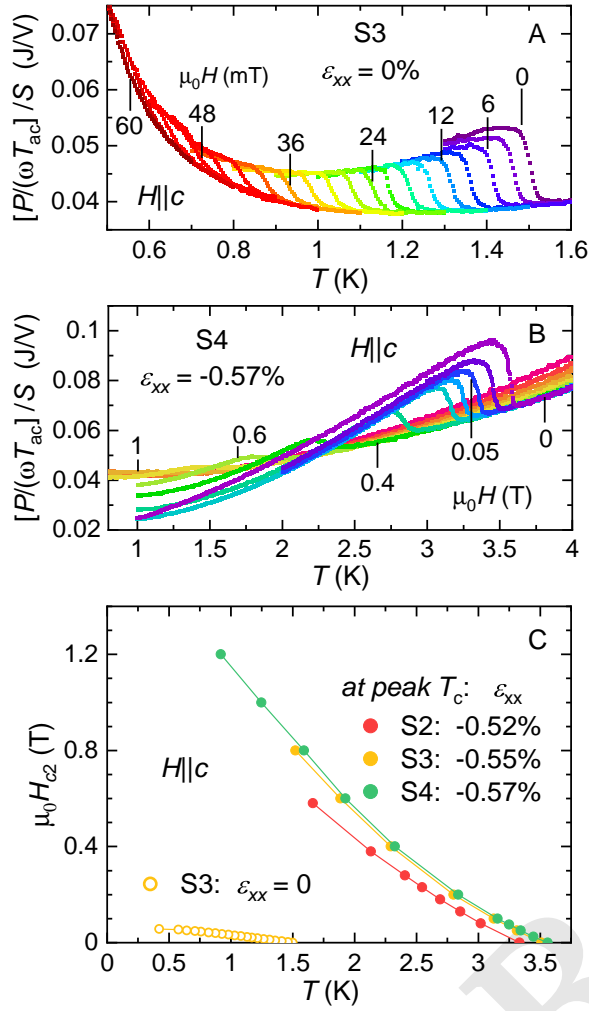


**Fig. 2.** (A) Experimental heat capacity data for magnetic fields  $\mu_0 H$  between zero and 60 mT at  $\varepsilon_{xx} = 0$  and (B)  $0 \leq \mu_0 H \leq 1$  T for 0.57% [panel (b)]. For explanation of the choice of plotted  $y$ -axis quantity see main text. (C) Critical fields as a function of temperature for sample S3 under zero strain and at its peak  $T_c$ , and for samples S2 and S4 at their peak values of  $T_c$ .

normalized by the Seebeck coefficient since the thermocouple is not calibrated in field. This does not have any influence on the position of the anomaly. The anomaly remains well-resolved over wide ranges of field, enabling the critical field curves to be deduced with confidence. Again, these are in good agreement with results previously obtained from magnetic susceptibility (28), and in particular confirm the slightly surprising observation that the shape of the critical field curves changes from the standard ‘convex’ curvature in unstrained material to a concave curvature when strained to the maximum  $T_c$ . The heat capacity measurements confirm that this is a bulk effect, and the data invite further theoretical attention.

As stated above, one of the naive expectations for two-component superconducting order parameters subject to uniaxial pressure is transition splitting. Heat capacity is a much more direct probe of such splitting than resistivity or magnetic susceptibility, because transitions in the superconducting state are not shorted or screened by the onset of the higher temperature superconducting phase. It is therefore particularly significant that there is no convincing qualitative evidence for

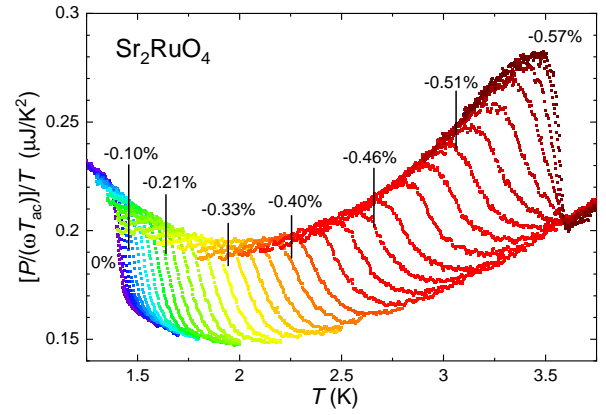


**Fig. 3.** (A) Experimental heat capacity data for sample S4 for thirty-six different strains between  $\varepsilon_{xx} = 0$  and (B)  $\varepsilon_{xx} = 0.57\%$ . For explanation of the choice of plotted  $y$ -axis quantity see main text.

such a splitting in our data, either as a function of strain or of magnetic field. We have checked this carefully with two further measurements. Firstly, we have carefully tracked the evolution of the leading edge of the anomaly with strain by sweeping the temperature through the transition at thirty-six distinct fixed strains, with the results displayed in Fig. 3. There is some transition broadening at intermediate strains, which can be understood because we have approximately 10% strain inhomogeneity across the probed portion of the sample, which broadens the observed transitions for the values of  $\varepsilon_{xx}$  for which  $dT_c/d\varepsilon_{xx}$  is large. We show all the actual data so that the readers can judge for themselves whether there is any clear evidence for splitting beyond this broadening; in our judgement there is none.

The second check that we have performed is explicitly informed by the findings that we reported in (23), in which muon-spin relaxation data indicate that the onset of time reversal symmetry breaking at  $T_{TRSB}$  occurs in the range 1.2 – 1.5 K for all strains lower than that at which  $T_c$  is maximized. By multiple averaging of data from the temperature range of interest, we reduced the r.m.s. voltage noise on the thermocouple signal to 0.5 pV, giving a detection limit for a sharp secondary transition of only 0.3% of the size of the primary one or, more realistically, a detection limit of 5% for a secondary transition of similar width to the that of the primary one (see *Supporting Information, Experimental Limits* for full details). Even the weaker 5% limit has strong implications for the underlying physics of  $\text{Sr}_2\text{RuO}_4$ , as we discuss below.

Before moving on to that discussion, we present our strain-dependent data after one step of processing, in order to gain further physical insight. Our measurement is not absolute, for the reasons described above, but it is possible to extract the ratio of the superconducting heat capacity to that in the normal state using a procedure (described in the *Supporting Information, Heat Capacity Jump*) that gives an accurate estimate of the normalized heat-capacity jump at  $T_c$  ( $\Delta c_s/c_n$ , where  $c_s$  and  $c_n$  are the heat capacities in the superconducting and normal states respectively) and is subject to error only at the level of tens of per cent for  $0.7T_c \leq T < T_c$ . The result of applying this analysis to data from a representative sample of  $\text{Sr}_2\text{RuO}_4$  is shown in Fig. 4. Importantly,  $\Delta c_s/c_n$  is seen to grow as the uniaxial pressure increases the superconducting

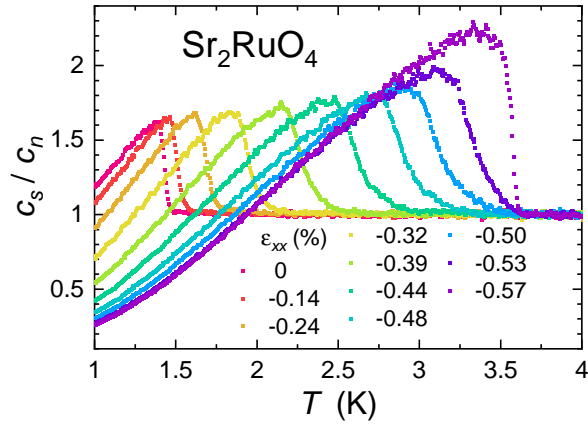


**Fig. 4.** Superconducting state heat capacity normalized to the normal-state value, showing the evolution of the anomaly height  $\Delta c_s/c_n$  with  $T_c$ . Data for the relative anomaly height are accurate, while the data below  $T_c$  are subject to small systematic errors described in the *Supporting Information, Heat Capacity Jump* (see also main text).

transition temperature. The significance of this observation is the following. There is now good evidence from calculations (28–30) and direct spectroscopic measurement (31) that the microscopic process that maximizes  $T_c$  in  $\text{Sr}_2\text{RuO}_4$  is tuning the Fermi level through a van Hove singularity, creating a pronounced maximum in the density of states. Within the two-dimensional Brillouin zone, the density of states is maximized near the zone boundary at the  $M$  point, so for any order parameter for which the gap has a symmetry-imposed zero at this point,  $\Delta c_s/c_n$  would naively be expected to fall, even as  $T_c$  was maximized. We observe the reverse effect, so our data are consistent with order parameters whose gap is allowed by symmetry to be maximal in this region of the Brillouin zone.

## Discussion

We close by discussing the relationship between our results and those obtained from other experiments, and the significance of our findings for the development of theory. The ultrasound measurements of (17, 18) probe another thermodynamic quantity, so one would expect consistency between the conclusions drawn there and the current findings. That is the case: the discontinuities observed in ultrasound velocity are consistent with transition splitting for pressure applied along the [110] direction, but no discontinuity was resolved in [100] modes. If the relevant physics is dominated by effects that are linear in strain couplings, the lack of splitting seen here as a function of [100] pressure is not in contradiction with those experiments. Future heat capacity work with pressure applied along [110] is desirable; in (18) the splitting  $T_c - T_{TRSB}$  is estimated to grow at a rate of at least 2 K/%-strain. In principle this could be resolved using our techniques.

In contrast to the ultrasound experiments,  $\mu\text{SR}$  does observe a split between the onset of spontaneous magnetism at  $T_{TRSB}$  and that of superconductivity at  $T_c$  in samples subject to [100] uniaxial pressure (23). One possibility for the apparent discrepancy between the two experiments is the inability of ultrasound measurements performed at MHz to resolve an attenuation discontinuity against the very large background attenuation seen in the [100] channel. This consideration would be particularly relevant if the thermodynamic

signature associated with the muon signal were very small. Our measurements confirm empirically that the latter is true: no heat capacity anomaly is observed at  $T_{TRSB}$  within conservative detection limits of 5% of the size of the anomaly at  $T_c$ . However, that does not remove the key challenge of reconciling such a small second anomaly with a TRSB state, for reasons we now outline.

The possible pairing states of the unstrained system can be naturally grouped into three categories: i)  $E$ -pairing, which is two-component and allows, alternatively, for time-reversal breaking  $E$ -pairing, such as  $d_{xz} \pm id_{yz}$ , for  $B_{2g}$ -nematic  $E$ -pairing  $d_{xz} \pm d_{yz}$ , or for  $B_{1g}$ -nematic  $E$ -pairing  $d_{xz}$  or  $d_{yz}$ , ii) two accidentally degenerate single component pairing states, such as  $d \pm ig$  or  $d \pm is$ , and iii) single component pairing such as the  $d_{x^2-y^2}$  state. While none of these states naturally accounts for all observations, our results offer strong evidence against some and give guidance which future experiments will allow to further discriminate between the remaining options for superconducting order.

A key finding of the  $\mu\text{SR}$  experiment is that the strain dependence of  $T_{TRSB}$  is much weaker than that of  $T_c$ . If we accept that odd parity order parameters are ruled out by the recent spin susceptibility experiments, the only even-parity state with a symmetry-protected degeneracy at  $T_c$ , i.e. the only even-parity candidate for non-accidental TRS breaking at  $T_c$  in unstrained  $\text{Sr}_2\text{RuO}_4$ , is  $E_g$ -pairing of the form  $d_{xz} + id_{yz}$  (32, 33). However, to leading order in strain, in Ginzburg-Landau theory such a state obeys the relationship that when the transition is split under uniaxial pressure, the ratio of the heat capacity anomaly jumps at the two transitions is inversely proportional to the strain dependences of the transition temperatures (for the derivation see the *Supporting Information, Heat Capacity Anomaly with  $E_g$  or  $E_u$  Pairing under Strain*). For  $\text{Sr}_2\text{RuO}_4$ , this would imply a larger heat capacity anomaly at  $T_{TRSB}$  than at  $T_c$ , in sharp contrast to our observations.

In Ref. (23), it was argued that the discrepancy between heat capacity ratios and  $T_c$  slopes could be explained by higher-order terms that dominate the leading order terms in the Ginzburg-Landau expansion even at relatively low strains. Here, we argue that although this is a reasonable hypothesis in the vicinity of the Lifshitz transition, where the evolution of the electronic structure is clearly nonlinear in strain, it appears less likely at low strains, and therefore that the absence of a resolvable second heat capacity anomaly makes TRSB  $E$ -pairing  $d_{xz} \pm id_{yz}$  order unlikely. The same is true for  $B_{2g}$ -nematic  $E$ -pairing with the additional problem that it does not account for time-reversal symmetry breaking.

For even parity superconductivity to be consistent with both the heat capacity and  $\mu\text{SR}$  it would need to involve some special tuning to yield the required exceptionally small heat capacity anomaly at  $T_{TRSB}$ . That naturally invites examination of states in which the degeneracy of the two components at  $T_c$  is accidental, and this relationship does not hold. A recently-proposed  $d + ig$  state (34) has the attractive feature that it predicts a pattern of ultrasound anomalies that is in agreement with experiment. However, the limit we place here on the size of the anomaly at  $T_{TRSB}$  is hard to reproduce (as the authors of (34) discuss). The problem of predicting a heat capacity anomaly at  $T_{TRSB}$  that is too large to be consistent with our experiments is even more pronounced for

theories involving other accidentally degenerate combinations of even parity states such as  $d + is$  (35), because unlike for the proposed  $d + ig$  state, the  $s$  component does not have a node in the same place as the  $d$  component. Intriguingly, a different postulate of a mixed parity order parameter with majority even and minority odd components (36) solves the problem of the lack of heat capacity anomaly at  $T_{TRSB}$  in a rather natural way. However, the predictions of that theory do not match the pattern of ultrasound anomalies and the theory is also strongly constrained by the newest NMR results (16).

Another possible avenue is worthy of consideration. The microscopic mechanism causing enhanced muon spin relaxation remains uncertain – scanned magnetic probe experiments do not resolve fields on the scale indicated by the muon spin relaxation – and so it in principle remains possible that the  $\mu$ SR results indicate some other transition in  $\text{Sr}_2\text{RuO}_4$  that is not related to the superconductivity. If the  $\mu$ SR data are neglected, then there are also several further possibilities. One is that transition splitting exists, but is much smaller under  $\langle 100 \rangle$  than  $\langle 110 \rangle$  uniaxial pressure, even as the van Hove singularity is approached. Notice this option is to leading order in strain not allowed for  $B_{2g}$ -nematic  $E$ -pairing or TRSB superconductivity in the  $E$ -representation. Another possibility is a  $B_{1g}$  nematic superconductor in the  $E$ -representation that yields a discontinuity of the elastic constants without split transitions or TRSB (17) (see also *Supporting Information, Heat Capacity Anomaly with  $E_g$  or  $E_u$  Pairing under Strain*). Such a state should be detectable via in-plane anisotropies below  $T_c$ , similar to the recently observed behavior in doped  $\text{Bi}_2\text{Se}_3$  (37–39).

A third possibility consistent with these heat capacity results considered in isolation is that the order parameter is single component at zero strain. However, this would require re-interpretation of both the recent  $\mu$ SR and ultrasound results; see Ref. (40) for a discussion.

## Conclusion

In summary, our comprehensive, high-resolution measurements of the heat capacity of  $\text{Sr}_2\text{RuO}_4$  as a function of strain, temperature and magnetic field confirm that previous susceptibility measurements were probing a bulk rather than a surface phenomenon. We do not resolve any signs of transition splitting of two order parameter components. Analysis of the data in comparison with recent findings from other thermodynamic and spectroscopic measurements places strong constraints on the search for a full theoretical explanation of its order parameter. Our results further guide that search by highlighting the importance of order parameters that can be maximal at the location of the van Hove singularity, and point to areas in which further experimental work is desirable.

## Materials and Methods

High-quality single-crystal  $\text{Sr}_2\text{RuO}_4$  samples were grown in a floating zone furnace (Canon Machinery) using techniques refined over many years to those described recently in (41). They were aligned using a bespoke Laue x-ray camera, and cut using a wire saw into thin bars with whose long axis aligned with the  $[100]$  direction of the crystal. For the best results these bars were polished using home-made apparatus based on diamond impregnated paper with a minimum grit size of  $1 \mu\text{m}$ . The bar was then mounted within

the jaws of a uniaxial pressure rig using Stycast 2850FT epoxy (Henkel Loctide). A resistive thin film resistor chip (State of the Art, Inc.) as heater and a calibrated Au-AuFe(0.07%) thermocouple were fixed to opposite sides of the sample using Dupont 6838 silver epoxy. Special care was taken when epoxying to the pressure cell to minimize tilt and ensure as homogeneous a strain field as possible. The uniaxial pressure apparatus was mounted on a dilution refrigerator, with thermal coupling to the mixing chamber via a high purity silver wire. The data shown in the paper were acquired between 500 mK and 4.2 K, with operation above 1.5 K achieved by circulating a small fraction of the mixture. The thermocouple was spot-welded in-house and its calibration fixed by reference to that of a calibrated  $\text{RuO}_2$  thermometer. The extremely low noise level of  $20 \text{ pVHz}^{-1/2}$  on the thermocouple readout was achieved by the combination of a low temperature transformer (CMR direct) mounted on the 1 K pot of the dilution refrigerator, operating at a gain of 300, and an EG&G 7265 lock-in amplifier. A Keithley 6221 low-noise current source was used to drive the heater. The piezo-electric actuators were driven at up to  $\pm 400 \text{ V}$  using a bespoke high-voltage amplifier. In a setup of this kind, the significance of heat leaks to the environment is gauged by the lower cut-off frequency of set-up response curves. By taking data at frequencies an order of magnitude higher than that lower cut-off, we ensure that the effect of such leaks makes a negligible contribution to our data. For further details on the technique see (26).

**ACKNOWLEDGMENTS.** We thank I. I. Mazin for useful discussions and R. Borth, M. Brando and U. Stockert for experimental support. Parts of this work were funded by the Deutsche Forschungsgemeinschaft (DFG, German Research Foundation) - TRR 288 - 422213477 (projects A10 and B01). NK acknowledges the support from JSPS KAKENHI (nos. JP17H06136 and JP18K04715) and JST-Mirai Program (no. JPMJMI18A3) in Japan and YM from JSPS KAKENHI (nos. JP15H05852, JP15K21717) and JSPS core-to-core programme. YSL acknowledges the support of a St Leonard’s scholarship from the University of St Andrews, the Engineering and Physical Sciences Research Council via the Scottish Condensed Matter Centre for Doctoral Training under grant EP/G03673X/1, and the Max Planck Society.

1. Maeno Y, et al. (1994) Superconductivity in a layered perovskite without copper. *Nature* 372:532–534.
2. Mackenzie AP, Maeno Y (2003) The superconductivity of  $\text{Sr}_2\text{RuO}_4$  and the physics of spin-triplet pairing. *Rev. Mod. Phys.* 75:657–712.
3. Mackenzie AP, et al. (1998) Extremely strong dependence of superconductivity on disorder in  $\text{Sr}_2\text{RuO}_4$ . *Phys. Rev. Lett.* 80:161–164.
4. Mackenzie AP, et al. (1996) Quantum oscillations in the layered perovskite superconductor  $\text{Sr}_2\text{RuO}_4$ . *Phys. Rev. Lett.* 76(20):3786–3789.
5. Maeno Y, et al. (1997) Two-dimensional Fermi liquid behavior of the superconductor  $\text{Sr}_2\text{RuO}_4$ . *J. Phys. Soc. Jpn.* 66(5):1405–1408.
6. Bergemann C, Julian SR, Mackenzie AP, NishiZaki S, Maeno Y (2000) Detailed topography of the Fermi surface of  $\text{Sr}_2\text{RuO}_4$ . *Phys. Rev. Lett.* 84(12):2662–2665.
7. Bergemann C, Mackenzie AP, Julian SR, Forsythe D, Ohmichi E (2003) Quasi-two-dimensional Fermi liquid properties of the unconventional superconductor  $\text{Sr}_2\text{RuO}_4$ . *Adv. Phys.* 52(7):639–725.
8. Raghu S, Kapitulnik A, Kivelson SA (2010) Hidden quasi-one-dimensional superconductivity in  $\text{Sr}_2\text{RuO}_4$ . *Phys. Rev. Lett.* 105:136401.
9. Scaffidi T, Romers JC, Simon SH (2014) Pairing symmetry and dominant band in  $\text{Sr}_2\text{RuO}_4$ . *Phys. Rev. B* 89:220510(R).
10. Reising HS, Scaffidi T, Flicker F, Lange GF, Simon SH (2019) Superconducting order of  $\text{Sr}_2\text{RuO}_4$  from a three-dimensional microscopic model. *Phys. Rev. Res.* 1(3):033108.
11. Mackenzie AP, Scaffidi T, Hicks CW, Maeno (2017) Even odder after twenty-three years: the superconducting order parameter puzzle of  $\text{Sr}_2\text{RuO}_4$ . *npj Quant. Mater.* 2:40.
12. Maeno Y, Kittaka S, Nomura T, Yonezawa S, Ishida K (2012) Evaluation of spin-triplet superconductivity in  $\text{Sr}_2\text{RuO}_4$ . *J. Phys. Soc. Jpn.* 81:11009.
13. Burganov B, et al. (2016) Strain control of fermiology and many-body interactions in two-dimensional ruthenates. *Phys. Rev. Lett.* 116:197003.
14. Pustogow A, et al. (2019) Constraints on the superconducting order parameter in  $\text{Sr}_2\text{RuO}_4$  from oxygen-17 nuclear magnetic resonance. *Nature* 574:72–75.
15. Ishida K, Manago M, Kinjo K, Maeno Y (2020) Reduction of the  $^{17}\text{O}$  Knight shift in the superconducting state and the heat-up effect by NMR pulses on  $\text{Sr}_2\text{RuO}_4$ . *J. Phys. Soc. Jpn.* 89(3):034712.
16. Chronister A, et al. (2020) Evidence for even parity unconventional superconductivity in  $\text{Sr}_2\text{RuO}_4$ . *arXiv* 2007.13730.

17. Benhabib S, et al. (2020) Ultrasound evidence for a two-component superconducting order parameter in  $\text{Sr}_2\text{RuO}_4$ . *Nat. Phys.* <https://doi.org/10.1038/s41567-020-1033-3>.
18. Ghosh S, et al. (2020) Thermodynamic evidence for a two-component superconducting order parameter in  $\text{Sr}_2\text{RuO}_4$ . *Nat. Phys.* <https://doi.org/10.1038/s41567-020-1032-4>.
19. Luke GM, et al. (1998) Time-reversal symmetry breaking superconductivity in  $\text{Sr}_2\text{RuO}_4$ . *Nature* 394:558–561.
20. Luke GM, et al. (2000) Unconventional superconductivity in  $\text{Sr}_2\text{RuO}_4$ . *Physica B* 289-290:373–376.
21. Xia J, Maeno Y, Beyersdorf PT, Fejer MM, Kapitulinik A (2006) High resolution polar kerr effect measurements of  $\text{Sr}_2\text{RuO}_4$ : Evidence for broken time-reversal symmetry in the superconducting state. *Phys. Rev. Lett.* 97:167002.
22. Sigrist M, Ueda K (1991) Phenomenological theory of unconventional superconductivity. *Rev. Mod. Phys.* 63:239–311.
23. Grinenko V, et al. (2020) Split superconducting and time-reversal symmetry-breaking transitions, and magnetic order in  $\text{Sr}_2\text{RuO}_4$  under uniaxial stress. *arXiv* 2001.08152.
24. Fisher RA, et al. (1989) Specific heat of  $\text{UPt}_3$ : Evidence for unconventional superconductivity. *Phys. Rev. Lett.* 62:1411–1414.
25. Hasselbach K, Taillefer L, Flouquet J (1989) Critical point in the superconducting phase diagram of  $\text{UPt}_3$ . *Phys. Rev. Lett.* 63(1):93–96.
26. Li YS, Borth R, Hicks CW, Mackenzie AP, Nicklas M (2020) Heat-capacity measurements under large uniaxial pressure using a piezo-driven device. *Rev. Sci. Instr.* 91:103903.
27. Hicks CW, et al. (2014) Strong increase of  $T_c$  of  $\text{Sr}_2\text{RuO}_4$  under both tensile and compressive strain. *Science* 344:283–285.
28. Steppke A, et al. (2017) Strong peak in  $T_c$  of  $\text{Sr}_2\text{RuO}_4$  under uniaxial pressure. *Science* 355.eaaf9398.
29. Hsu YT, et al. (2016) Manipulating superconductivity in ruthenates through Fermi surface engineering. *Phys. Rev. B* 94:045118.
30. Barber ME, et al. (2019) Role of correlations in determining the van Hove strain in  $\text{Sr}_2\text{RuO}_4$ . *Phys. Rev. B* 100(24):245139.
31. Sunko V, et al. (2019) Direct observation of a uniaxial stress-driven Lifshitz transition in  $\text{Sr}_2\text{RuO}_4$ . *npj Quant. Mat.* 4:2397–4648.
32. Žutić I, Mazin I (2005) Phase-sensitive tests of the pairing state symmetry in  $\text{Sr}_2\text{RuO}_4$ . *Phys. Rev. Lett.* 95:217004.
33. Suh HG, et al. (2020) Stabilizing even-parity chiral superconductivity in  $\text{Sr}_2\text{RuO}_4$ . *Phys. Rev. Res.* 2:032023(R).
34. Kivelson SA, Yuan AC, Ramshaw BJ, Thomale R (2020) A proposal for reconciling diverse experiments on the superconducting state in  $\text{Sr}_2\text{RuO}_4$ . *npj Quant. Mater.* 5:43.
35. Römer AT, Scherer DD, Eremin IM, Hirschfeld PJ, Andersen BM (2019) Knight shift and leading superconducting instability from spin fluctuations in  $\text{Sr}_2\text{RuO}_4$ . *Phys. Rev. Lett.* 123:247001.
36. Scaffidi T (2020) Degeneracy between even- and odd-parity superconductivity in the quasi-1D Hubbard model and implications for  $\text{Sr}_2\text{RuO}_4$ . *arXiv* 2007.13769.
37. Matano K, Kriener M, Segawa K, Ando Y, Zheng Gq (2016) Spin-rotation symmetry breaking in the superconducting state of  $\text{Cu}_x\text{Bi}_2\text{Se}_3$ . *Nat. Phys.* 12:852—854.
38. Yonezawa S, et al. (2017) Thermodynamic evidence for nematic superconductivity in  $\text{Cu}_x\text{Bi}_2\text{Se}_3$ . *Nat. Phys.* 13:123–126.
39. Cho Cw, et al. (2020)  $\mathbb{Z}_3$ -vestigial nematic order due to superconducting fluctuations in the doped topological insulators  $\text{Nb}_x\text{Bi}_2\text{Se}_3$  and  $\text{Cu}_x\text{Bi}_2\text{Se}_3$ . *Nat. Commun.* 11:3056.
40. Willa R, Hecker M, Fernandes RM, Schmalian J (2020) Inhomogeneous time-reversal symmetry breaking in  $\text{Sr}_2\text{RuO}_4$ . *arXiv* 2011.01941.
41. Bobowski JS, et al. (2019) Improved single-crystal growth of  $\text{Sr}_2\text{RuO}_4$ . *Condens. Matter* 4:6.